

Integrating UAVs as Transparent Relays into Mobile Networks: A Deep Learning Approach

Mehyar Najla [†], Zdenek Becvar [†], Pavel Mach [†], and David Gesbert ^{*}

[†] Dpt. of Telecommunication Engineering, FEE, Czech Technical University in Prague, Prague, Czech republic

^{*} Communication Systems Department, EURECOM, Sophia Antipolis, France

emails: [†] {najlameh, zdenek.becvar, machp2}@fel.cvut.cz, ^{*} gesbert@eurecom.fr

Abstract—Since flying base stations (FlyBSs) are energy constrained, it is convenient for them to act as transparent relays with minimal communication control and management functionalities. The challenge when using the transparent relays is the inability to measure the relaying channel quality between the relay and user equipment (UE). This channel quality information is required for communication-related functions, such as the UE association, however, this information is not available to the network. In this letter, we show that it is possible to determine the UEs' association based only on the information commonly available to the network, i.e., the quality of the cellular channels between conventional static base stations (SBSs) and the UEs. Our proposed association scheme is implemented through deep neural networks, which capitalize on the mutual relation between the unknown relaying channel from any UE to the FlyBS and the known cellular channels from this UE to multiple surrounding SBSs. We demonstrate that our proposed framework yields a sum capacity that is close to the capacity reached by solving the association via exhaustive search.

Index Terms—Unmanned Aerial Vehicles, transparent relays, users' association, deep neural networks

I. INTRODUCTION

Unmanned Aerial Vehicles (UAVs) are expected to be integrated in future mobile networks as flying base stations (FlyBSs) complementing conventional static base stations (SBS) in some areas of the network, at the time when the high density of users and the dynamicity of the network are difficult to adapt to with a purely fixed infrastructure [1]. In such scenarios, the FlyBS relays the communication between the conventional SBS and the user equipment (UE).

The relays can be classified into non-transparent and transparent [2]. The non-transparent relays are distinguished by their high complexity as these are supposed to perform all the communication-related functions, such as data processing, radio resource management, or signaling, in a similar way as the conventional SBSs [3]. In contrast, the transparent relays represent a simplified and a lightweight version of the relays, for which the majority of the communication functions are managed centrally by the conventional SBS [4]. Consequently, the transparent relays are significantly cheaper and less energy

demanding in comparison to the non-transparent relays as that transparent type requires less complex hardware [2]. Since the energy consumption of the FlyBSs is directly proportional to their operational time, the transparent relays are seen as suitable and convenient candidates for the FlyBSs.

To this end, the main obstacle facing the deployment of the FlyBSs acting as transparent relays arises from the fact that the transparent relays are not able to obtain the information about the quality of the channels between the UEs and the FlyBSs due to their simple nature. The reason is that the transparent relays do not transmit their own reference signals, which are required to determine the channel quality (see, e.g., [4], [5]). To solve this problem, the statistical channel gains between the UEs and the FlyBSs can be derived based on the existing path loss models. Nevertheless, these statistical channel gains rely on the knowledge of UEs' locations [6]-[8] or, at least, on the knowledge of the spatial distribution of UEs [9]-[10]. However, the information about the UEs' locations might not be available to the network due to the privacy preferences or the specific location of the user (e.g., the UE is at a place where no localization system is available). In such case, it is hard to decide whether to associate the UEs to a specific FlyBS or directly to the SBS.

In this paper, we focus on the case where the FlyBSs represent transparent relays, and we target the problem of the inability of the transparent FlyBSs to measure the channel gains between the UEs and the FlyBSs for the UEs' association. We also consider a practical scenario where an arbitrary part of the UEs makes their locations available to the network while another part of the UEs do not disclose their locations. To this end, we propose a deep neural network (DNN) that is able to predict the association of the UEs not disclosing their locations neither to the SBS nor to one of the FlyBSs. The objective is to maximize the sum capacity of these UEs. The UEs' association is predicted by the DNN based only on the knowledge of information commonly available to the network: 1) the quality of cellular channels between the UEs and the surrounding SBSs (note that the qualities of cellular channels are reported periodically in common networks [11], e.g., for handover purposes), 2) the FlyBSs' positions, which are known for the FlyBSs' navigation purposes, and 3) the number of the UEs already attached to each base station

This work has been supported by Grant No. P102-18-27023S funded by Czech Science Foundation and by the project of Czech Technical University in Prague no. SGS20/169/OHK3/3T/13.

978-1-7281-4490-0/20/\$31.00 © 2020 IEEE

(BS) as this number affects the resource allocation at the BSs (this information is known a priori for general radio resource management purposes). The DNN is trained offline and, then, exploited to associate the UEs. The DNN ability to make the association decision instantaneously is a significant asset of the proposed scheme from the practical implementation point of view in the real mobile network.

The rest of the paper is organized as follows. In Section II, the system model is presented and the targeted optimization problem is formulated. Then, in Section III, the proposed DNN-based scheme for UEs' association is described in detail. Section IV presents the simulation scenarios and discusses the results. Finally, Section V concludes the paper.

II. SYSTEM MODEL AND PROBLEM FORMULATION

We consider a set \mathcal{N} containing $|\mathcal{N}|$ uniformly deployed UEs with their locations known to the network. In addition, there exist another set \mathcal{M} of $|\mathcal{M}|$ uniformly deployed UEs for which the locations are not known. All UEs are deployed within a single cell and belong to a set \mathcal{U} of $|\mathcal{U}|$ UEs where $\mathcal{U} = \mathcal{N} \cup \mathcal{M}$, $\mathcal{N} \cap \mathcal{M} = \emptyset$, and $|\mathcal{U}| = |\mathcal{N}| + |\mathcal{M}|$. The UEs are served by $|\mathcal{L}|$ BSs included in a set \mathcal{L} , encompassing one SBS and $|\mathcal{L}|-1$ FlyBSs acting as the transparent relays (note that, in this paper, the BS denotes arbitrary type of base station including SBS as well as FlyBS). Without loss of generality, we assume that all UEs communicate in the downlink direction. As in [12], the 2D positions (i.e., with fixed altitude) of the FlyBSs are determined with respect to the known locations of the UEs from \mathcal{N} via K-means. Note that, while the association of the UEs from \mathcal{N} is done based on their known locations (as in [12]), the association of the UEs with unknown locations from \mathcal{M} is the targeted problem in this paper. Although we focus specifically on a single cell, there is also a set \mathcal{K} of $|\mathcal{K}|$ SBSs in the vicinity. The qualities of the channels between every UE and all the $|\mathcal{K}|$ neighboring SBSs are measured and reported periodically as in conventional mobile networks, e.g., for mobility management and handover purposes.

Without loss of generality, we assume that the deployed $|\mathcal{K}|+1$ SBSs use orthogonal bandwidths (i.e., every SBS exploits its own dedicated bandwidth). In contrast, all FlyBSs reuse the same bandwidth B of their serving SBS to ensure a high spectral efficiency (see Fig. 1). The serving SBS divides the whole bandwidth B equally among all served UEs. The UE communicates either directly with the SBS (via direct channel from the SBS to the UE) or via the FlyBS (occupying the backhaul channel from the SBS to the FlyBS and the channel from the FlyBS to the UE). Note that the bandwidth allocation to individual UEs for the communication from the FlyBS to the UE is determined by the SBS as the FlyBSs represent transparent relays with limited functionalities. Further, every FlyBS is able to receive and transmit data at the same time. Since the same bandwidth is reused by all BSs, communication of each FlyBS with the SBS over backhaul is exposed to an interference induced by other FlyBSs. Similarly, each UE

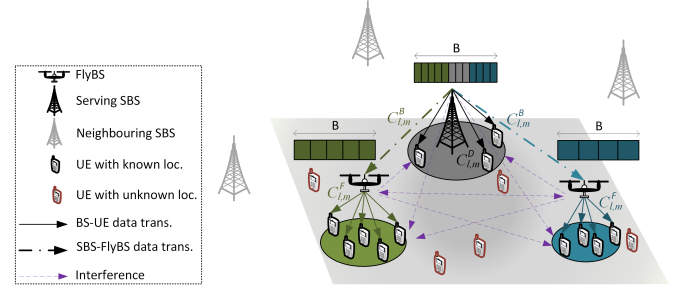


Fig. 1: System model.

experiences an interference from all BSs (either SBS or FlyBS) except the serving one.

If the m -th UE from \mathcal{M} is served directly by the SBS, its capacity $C_{l,m}^D$ is defined as:

$$C_{l,m}^D = \frac{B}{|\mathcal{U}|} \log_2 \left(1 + \frac{\frac{p_1}{|\mathcal{U}|} g_{1,m}}{\frac{B}{|\mathcal{U}|} \sigma + \sum_{l=2}^{|\mathcal{L}|} \frac{p_l}{|\mathcal{U}|} g_{l,m}} \right) \quad (1)$$

where p_l is the transmission power of the l -th BS over the whole allocated bandwidth, $g_{l,m}$ is the channel gain between the l -th BS and the m -th UE, and σ is the noise spectral density. Note that $l=1$ refers to the serving SBS and, thus, p_1 and $g_{1,m}$ are the transmission power of the serving SBS and the channel gain between this SBS and the m -th UE. Moreover, in (1), we see that all FlyBSs cause interference to the m -th UE if this UE is associated directly to the serving SBS.

If the m -th UE is attached to the SBS through an intermediate FlyBS, the backhaul capacity $C_{l,m}^B$ (between the SBS and the relaying FlyBS) is calculated as:

$$C_{l,m}^B = \frac{B}{|\mathcal{U}|} \log_2 \left(1 + \frac{\frac{p_1}{|\mathcal{U}|} g_{1,l}}{\frac{B}{|\mathcal{U}|} \sigma + \sum_{\substack{i \neq l \\ i=2}}^{|\mathcal{L}|} \frac{p_i}{|\mathcal{U}|} g_{i,l}} \right) \quad (2)$$

where $g_{1,l}$ is the channel gain between the serving SBS and the l -th FlyBS to which the m -th UE is attached, and $g_{i,l}$ is the interference channel gain between the i -th FlyBS inducing the interference and the l -th FlyBS through which the m -th UE is served. Similarly, the capacity $C_{l,m}^F$ of the channel between the l -th FlyBS and the m -th UE is derived as:

$$C_{l,m}^F = \frac{B}{n_l} \log_2 \left(1 + \frac{\frac{p_l}{n_l} g_{l,m}}{\frac{B}{n_l} \sigma + \sum_{\substack{i \neq l \\ i=1}}^{|\mathcal{L}|} \frac{p_i}{n_l} g_{i,m}} \right) \quad (3)$$

where n_l is the number of all UEs from \mathcal{U} associated to the l -th FlyBS (i.e., $n_l \leq |\mathcal{U}|$), $g_{l,m}$ is the channel gain between the l -th FlyBS and the m -th UE attached to it, and $g_{i,m}$ is the interference caused by the i -th BS to the m -th UE.

Then, the capacity of the m -th UE associated to the l -th

FlyBS is derived as:

$$C_{l,m} = \begin{cases} C_{l,m}^D & \text{if } l = 1 \\ \min(C_{l,m}^B, C_{l,m}^F) & \text{if } l > 1 \end{cases} \quad (4)$$

In order to define whether the m -th UE is associated to the SBS or to one of the FlyBSs, we introduce the association matrix α expressed as:

$$\alpha = \begin{bmatrix} \alpha_1^1 & \dots & \alpha_1^{|\mathcal{L}|} \\ \vdots & \ddots & \vdots \\ \alpha_{|\mathcal{M}|}^1 & \dots & \alpha_{|\mathcal{M}|}^{|\mathcal{L}|} \end{bmatrix} \quad (5)$$

where $\alpha_m^l = 1$ indicates that the m -th UE is associated to the l -th BS, otherwise α_m^l is set to 0. Taking this into consideration, n_l in (3) is calculated as:

$$n_l = N_l + \sum_{m=1}^{m=|\mathcal{M}|} \alpha_m^l \quad (6)$$

where N_l is the number of the UEs from \mathcal{N} that are attached to the l -th FlyBS and $\sum_{m=1}^{m=|\mathcal{M}|} \alpha_m^l$ represents the number of UEs from \mathcal{M} that become attached to the l -th FlyBS.

Based on (1)-(6), the mathematical formulation of the problem of maximizing the sum capacity of the UEs with unknown locations (i.e., the $|\mathcal{M}|$ UEs from \mathcal{M}), is written as:

$$\begin{aligned} \alpha^* &= \underset{\alpha}{\operatorname{argmax}} \left(\sum_{m=1}^{m=|\mathcal{M}|} \sum_{l=1}^{l=|\mathcal{L}|} \alpha_m^l C_m^l \right) \quad (7) \\ \text{s.t.} \quad & \sum_{l=1}^{l=|\mathcal{L}|} \alpha_m^l = 1 \quad \forall m \in \mathcal{M} \quad (a) \end{aligned}$$

where α^* represents the targeted α that maximizes the sum capacity of the $|\mathcal{M}|$ UEs, and the constraint (a) guarantees that each UE is associated to only one BS at a time.

The solution of the problem presented in (7) is not only affected by the quality of the channels between the $|\mathcal{M}|$ UEs and the $|\mathcal{L}|$ BSs, but it is also influenced by the bandwidth allocation for each UE at individual BSs as the bandwidth allocation changes with the association. In addition, the bandwidth splitting is also affected by the number of UEs attached to each BS. Moreover, C_m^l is a function of n_l , which is a function of α as shown in (6). Thus, the problem in (7) is an integer non-linear programming problem that is known to be NP-hard. Such problem can be generally solved by an exhaustive search. Nevertheless, the absence of the information on the locations of the $|\mathcal{M}|$ UEs as well as the FlyBSs' inability to measure the channel quality between themselves and the $|\mathcal{M}|$ UEs *make the problem unsolvable* in real networks *even with the exhaustive search*. Thus, in the next section, we rely only on the commonly known and periodically measured (and reported) cellular channel gains between the $|\mathcal{M}|$ UEs and the serving SBS together with K surrounding SBSs to design the DNN that is able to make an instantaneous decision on the association of the $|\mathcal{M}|$ UEs whose locations are not known.

III. PROPOSED ASSOCIATION OF UES IN NETWORKS WITH TRANSPARENT RELAYS

In this section, we, first, explain the principle of the proposed UEs' association scheme based on the cellular channels. Then, the proposed DNN architecture, training and exploitation in real mobile networks are explained.

A. Principle of cellular channels-based UEs' association

Generally, when the FlyBSs act as the transparent relays, the relaying channels between the UEs and those FlyBSs cannot be estimated as explained in Section I. Hence, to associate the UEs from \mathcal{M} , an exploitation of the statistical channel gains derived based on existing channel models is the only known solution. Still, the statistical channel gain between any UE and the FlyBS with the existing channel models can be determined only if the locations of both the UE and the FlyBS are known. However, the locations of the UEs from \mathcal{M} are not available and the problem should be circumvented by an exploitation of another available information about these UEs. In fact, the cellular channels between any UE and the surrounding SBSs are commonly known as these cellular channels are measured and reported periodically for, e.g., mobility management and handover purposes. In an open field, a single UE can be distinguished by the cellular channels from this UE to the surrounding (neighboring) SBSs. Therefore, for the UEs with unknown locations from \mathcal{M} , the cellular channels between these UEs and multiple surrounding SBSs are seen as a proper substitution of the missing information on the channels to the FlyBSs taking into account that the positions of these FlyBSs are known.

Based on this principle, the problem presented in (7), can be solved knowing: i) the cellular channels between the UEs and multiple neighboring SBSs (reported periodically), ii) the FlyBSs' positions (known for the FlyBSs' navigation), and iii) the number of UEs from \mathcal{N} attached to every BS, i.e., every $N_l \forall l \in \mathcal{L}$ from (6) (this information affects the bandwidth splitting at the BSs and it is known by network operator as the resource allocation for all FlyBSs is done by the serving SBS). Nevertheless, the mapping between this available information (UEs' cellular gains, FlyBSs' locations, the number of the UEs attached to every BS) and the optimal association of the UEs from \mathcal{M} is not known and cannot be analytically derived. Hence, we train the DNN to build the mapping between the pre-mentioned available information and the optimal association of the $|\mathcal{M}|$ UEs with unknown locations. This trained DNN is stored at the serving SBS, which decides and controls the association of all $|\mathcal{M}|$ UEs to the SBS or to one of the FlyBSs.

B. Architecture of proposed DNN

The association of every UE from \mathcal{M} to one of the $|\mathcal{L}|$ BSs can be seen as $|\mathcal{M}|$ identical classification problems. Thus, we train one DNN for multi-class classification in order to predict the association of any m -th UE from \mathcal{M} to either the serving SBS or to one of the FlyBSs. Then, the trained DNN is exploited to predict the association of every UE at the

same time in parallel (details are explained later in Section III-C). The architecture of the DNN includes one input layer, H hidden layers, and finally a SOFTMAX layer serving as the output layer (see Fig. 2).

The input vector \mathbf{I}_1 , which represents the input layer, is composed of three parts \mathbf{I}_1^1 , \mathbf{I}_1^2 and \mathbf{I}_1^3 . The first part provides the DNN with the information regarding the cellular channel gains of all $|\mathcal{M}|$ UEs to every SBS in proximity to these UEs. Thus, the length of the first part \mathbf{I}_1^1 of the DNN's input is equal to the number of the reported/known UEs' cellular gains, i.e.:

$$|\mathbf{I}_1^1| = (|\mathcal{K}|+1)|\mathcal{M}| \quad (8)$$

The second part \mathbf{I}_1^2 of the input expresses the locations of individual FlyBSs under the SBS coverage, thus, the length of this second part is:

$$|\mathbf{I}_1^2| = 3(|\mathcal{L}|-1) \quad (9)$$

where the number "3" represents three coordinates of each FlyBS in 3D space. The third part \mathbf{I}_1^3 , constituting the DNN input, corresponds to the number of the UEs from \mathcal{N} already attached to each BS. Hence, the length of this third part is:

$$|\mathbf{I}_1^3| = |\mathcal{L}| \quad (10)$$

As a result, the input vector of DNN is of a length:

$$|\mathbf{I}_1| = |\mathbf{I}_1^1| + |\mathbf{I}_1^2| + |\mathbf{I}_1^3| = (|\mathcal{K}|+1)|\mathcal{M}| + 3(|\mathcal{L}|-1) + |\mathcal{L}| \quad (11)$$

The DNN input \mathbf{I}_1 is followed by H sequential hidden layers. Consequently, \mathbf{I}_1 is the input of the first hidden layer h_1 . Then, the input of any other hidden layer is, at the same time, the output of the previous hidden layer. Every hidden layer h_j is composed of X_j neurons, where each input element from the inputs of h_j is fed to each of these X_j neurons with a corresponding weight. In every neuron in the layer h_j , the dot product between the inputs of h_j and the corresponding weights is performed. Then, the neuron adds its bias to the result of the dot product and implements the sigmoid activation function resulting in the neuron's output (i.e., a single value). Thus, the output of any hidden layer h_j with X_j neurons is a vector of a length X_j , and this output is calculated as:

$$\mathbf{O}_j = \text{sig}(\mathbf{W}_j \cdot \mathbf{I}_j + \mathbf{b}_j) \quad (12)$$

where $\text{sig}(\cdot)$ is the sigmoid function such that $\text{sig}(\gamma) = \frac{1}{1+\exp(-\gamma)}$, \mathbf{I}_j is the vector that contains the inputs of the hidden layer h_j , \mathbf{W}_j is the matrix containing the weights of the links connecting every input in \mathbf{I}_j and every neuron in h_j , and \mathbf{b}_j represents the vector that includes the biases of the X_j neurons in h_j .

The output vector of the last hidden layer (i.e., the vector \mathbf{O}_H from (12) with $j = H$ representing the last hidden layer) is the input of the SOFTMAX output layer. The SOFTMAX layer is composed of $|\mathcal{L}|$ neurons as the number of classes in our problem is also $|\mathcal{L}|$ (i.e., the number of available options for the association of the m -th UE). Every neuron l in the SOFTMAX layer implements the dot product between \mathbf{O}_H and

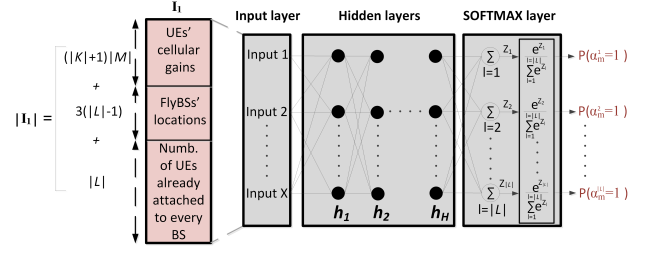


Fig. 2: Proposed DNN to predict the association of a single UE from \mathcal{M} .

the corresponding weights and adds the corresponding bias, resulting in the value Z_l . Hence, considering all the $|\mathcal{L}|$ neurons in the SOFTMAX layer, we get the vector \mathbf{Z} of a length $|\mathcal{L}|$, such that $\mathbf{Z} = \{Z_1, Z_2, \dots, Z_{|\mathcal{L}|}\}$. Finally, the elements in \mathbf{Z} are inserted to the SOFTMAX function giving, for every element Z_l with $l \in \mathcal{L}$, a final single output $P(\alpha_m^l)$. Note that $P(\alpha_m^l)$ represents the probability of the m -th UE being associated to the l -th BS (the probability that $\alpha_m^l = 1$). This probability is calculated as:

$$P(\alpha_m^l) = \frac{\exp(Z_l)}{\sum_{l=1}^{|\mathcal{L}|} \exp(Z_l)} \quad (13)$$

From (13), we see that $\sum_{l=1}^{|\mathcal{L}|} P(\alpha_m^l) = 1$. Hence, the final chosen association for the m -th UE is:

$$\alpha_m^l = \begin{cases} 1 & \text{if } P(\alpha_m^l) > P(\alpha_m^q) \forall q \in \mathcal{L}/\{l\} \\ 0 & \text{otherwise} \end{cases} \quad (14)$$

C. Training and exploitation of proposed DNN for UEs' association

The proposed DNN utilizes supervised learning approach trying to reach a specific target. In our case, the target is derived by the exhaustive search when all possible association combinations for $|\mathcal{M}|$ UEs (i.e., $|\mathcal{L}|^{|\mathcal{M}|}$ combinations) are checked and the one yielding the highest sum capacity is selected as the optimal association combination. Then, for any m -th UE from the $|\mathcal{M}|$ UEs (e.g., the first UE in \mathcal{M}), the index of the chosen BS (i.e., l^* where $l^* \in \mathcal{L}$) is considered as the target that the DNN aims to predict. To that end, the learning process starts with collecting a set of training samples, e.g., by simulating the targeted area and scenario. Each sample represents a single simulation drop and includes the set of available information (i.e., the information feed to the input of the DNN described in Section III-B) as features and the corresponding target. Then, the features of each sample are inserted to the DNN with randomly set weights and biases giving, at its output, the association of the m -th UE. Next, the comparison between the DNN output and the targeted output for each sample is performed via cross-entropy loss function

written as:

$$\delta = - \sum_{l=1}^{l=|\mathcal{L}|} [l^* == l] \log(P(\alpha_m^l)) \quad (15)$$

The cross-entropy loss function averaged over the training samples is minimized by subsequent updating of the weights and the biases of the DNN via the scaled-conjugate gradient back-propagation [13]. Then, a new training iteration is performed with the updated weights and biases. The training process is terminated if the number of iterations exceeds the maximal number of iterations or if the prediction accuracy increment from one iteration to another becomes very small.

Key benefit of the proposed solution is that the training process is performed offline and there is no training needed online in the real mobile network. Then, in the real mobile network, the same already trained DNN is exploited to instantly determine the optimal association of every UE from the $|\mathcal{M}|$ UEs simultaneously. For example, consider that the DNN is trained to predict the optimal association for the first UE from \mathcal{M} (the UE for which the cellular gains are put at the beginning of \mathbf{I}_1). In such case, to predict the optimal association for the second UE, we put the cellular gains of this second UE at the beginning of \mathbf{I}_1 .

IV. PERFORMANCE ANALYSIS

The simulations are done in MATLAB considering a 500×500 m area within which $|\mathcal{N}|=10$ UEs with known locations and up to $|\mathcal{M}|=5$ UEs with unknown locations are uniformly deployed. The area contains also one serving SBS deployed in the middle of the area and two FlyBSs acting as transparent relays (as shown in Fig. 1). In addition to the serving SBS, we assume $|\mathcal{K}|=2, 3$, or 4 additional SBSs in the neighboring areas with fixed uniformly generated locations. We consider that the $|\mathcal{N}|$ UEs with known locations are already associated to the serving SBS either directly or through one of the two available FlyBSs, while the $|\mathcal{M}|$ UEs with unknown locations are, then, associated based on the proposed scheme illustrated in Section III. The height and the transmission power (over

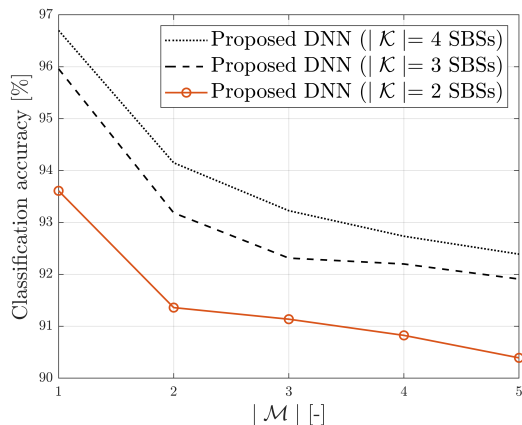


Fig. 3: Classification accuracy vs $|\mathcal{M}|$.

all channels) p_l of each BS are set to 30 m and 27 dBm, respectively. The total bandwidth B reused by every BS is set to 20 MHz. The gains of the channels between the FlyBSs and the UEs, between the SBS and the UEs, and between the SBS and the FlyBSs are generated in line with path loss models from [14] with 2 GHz carrier frequency.

Note that the DNN is trained for each value of $|\mathcal{M}|$ separately, and with a total number of collected samples equal to 3×10^5 . Note that the number of samples is set by trial and error approach and the learning accuracy increment is negligible for larger numbers of samples.

Fig. 3 shows the DNN prediction accuracy (the percentage of the DNN's outputs that match the optimal targeted association) versus different numbers of UEs in \mathcal{M} and for different numbers of available neighboring SBSs (i.e., $|\mathcal{K}|$). As expected, with the increasing number of SBSs the prediction accuracy is increasing as the DNN is able to better learn the scenario layout. Thus, if four SBSs are in vicinity (in addition to the serving one), the accuracy varies between 92.5% (for $|\mathcal{M}|=1$) and 96.7% (for $|\mathcal{M}|=5$). Still, even for a lower number of SBSs (i.e., $|\mathcal{K}|=2$ or $|\mathcal{K}|=3$), the prediction accuracy is always higher than 90%. Fig. 3 further demonstrates that the prediction accuracy decreases with the increasing $|\mathcal{M}|$ due to the growing complexity of the association problem (more UEs need to be associated with different channels and bandwidth splitting options).

Fig. 4 illustrates the sum capacity of the $|\mathcal{M}|$ UEs if $|\mathcal{K}|=2$. To the best of our knowledge, there is no existing work that solves the UEs' association for the case when both the UEs' locations as well as the relaying channels between the FlyBSs (acting as the transparent relays) and the UEs are absent. Thus, the proposed DNN is compared to the following association schemes: 1) Optimal association derived by the exhaustive search (in the figure denoted as *Optimum*), 2) Random association where each UE is associated with equal probability to the serving SBS or one of the FlyBSs (denoted as *Random*), 3) all UEs are associated to one of the FlyBS (denoted as *Only FlyBS*), and 4) all UEs are associated to the serving SBS (denoted as *Only SBS*). Note that *Optimum* is not derivable

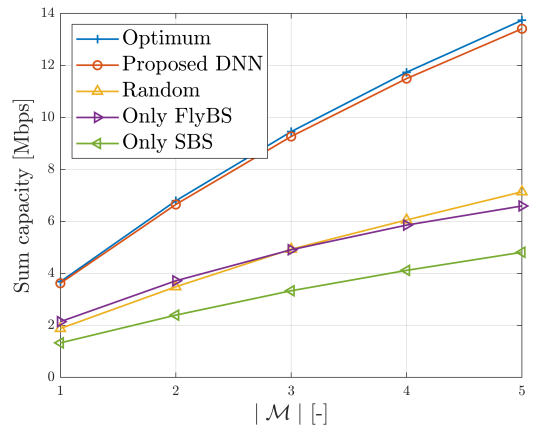


Fig. 4: Sum capacity of the $|\mathcal{M}|$ UEs for $|\mathcal{K}|=2$.

in real networks with the FlyBSs acting as transparent relays and the locations of the $|\mathcal{M}|$ UEs being unknown. In this paper, we depict *Optimum* only for benchmarking purposes.

Fig. 4 demonstrates that the proposed scheme, with only three SBSs ($|\mathcal{K}|=2$ neighboring SBSs plus the serving SBS), reaches a close-to-optimal sum capacity with a loss with respect to the optimum always below 2.4%. Moreover, the sum capacity reached by the proposed scheme with respect to the capacity of the other three association schemes is increased by up to 91%, 103%, and 280% when compared to *Random*, *Only FlyBS* and *Only SBS*, respectively.

V. CONCLUSIONS

In this paper, we have proposed a novel DNN-based framework to determine the association of the UEs with unknown locations either to the serving SBS or to one of the FlyBSs acting as the transparent relays. The transparent relay mode for the FlyBSs is selected as the transparent relays are lighter, less expensive, and consume less energy comparing to the non-transparent ones. This makes the transparent relays suitable for FlyBSs. To this end, we exploit the knowledge of cellular channels between the UEs and the surrounding SBS to overcome the problem of the transparent relays' inability to measure the quality of the channels between themselves and the UEs as well as the absence of the UEs' location information. By knowing the UEs' periodically reported cellular channels, our proposed DNN determines the UEs' association maximizing their sum capacity. The results confirm the close-to-optimal performance of our proposal.

REFERENCES

- [1] Y. Zeng, et al., "Wireless communications with unmanned aerial vehicles: Opportunities and challenges," *IEEE Communications Magazine*, 54(5), pp. 36–42, 2016.
- [2] Huawei, "Understanding on Type 1 and Type 2 Relay," *3GPP TSG RAN WG1 Meeting #57bis*, Los Angeles, USA, June 29- July3, 2009 (R1 092370).
- [3] C. Hoymann, et al., "Relaying operation in GPP LTE: challenges and solutions," *IEEE Communications Magazine*, 50(2), pp. 156–162, 2012.
- [4] Motorola, "Discussion of Type II (Transparent) Relays for LTE," *3GPP TSG RAN WG1 Meeting #57*, San Francisco, USA, May 4-8, 2009 (R1 091941).
- [5] Huawei, "Issues of Type 2 Relay," *3GPP TSG RAN WG1 Meeting #57bis*, Los Angeles, USA, June 29- July3, 2009 (R1 092372).
- [6] J. Chen, et al., "Optimal positioning of flying relays for wireless networks: A LOS map approach," *IEEE international conference on communications (ICC)*, pp. 1–6, 2017.
- [7] M. Alzenad, et al., "3-D placement of an unmanned aerial vehicle base station for maximum coverage of users with different QoS requirements," *IEEE Wireless Communication Letters*, 7(1), pp. 38–41, 2016.
- [8] J. Plachy, et al., "Joint positioning of Flying Base stations and Association of Users: Evolutionary-based approach," *IEEE Access*, 7, pp. 11454–11463, 2019.
- [9] M. Mozaffari, et al., "Optimal transport theory for cell association in UAV-enabled cellular networks," *IEEE Communications Letters*, 21(9), pp. 2053–2056, 2017.
- [10] M. Mozaffari, et al., "Wireless communication using unmanned aerial vehicles (UAVs): Optimal transport theory for hover time optimization," *IEEE Transactions on Wireless Communications*, 16(12), pp. 8052–8066, 2017.
- [11] D. Astely, et al., "LTE: the evolution of mobile broadband," *IEEE Communications Magazine*, 47(4), pp. 44–51, 2009.
- [12] B. Galkin, et al., "Deployment of UAV-mounted access points according to spatial user locations in two-tier cellular networks," *Wireless Days (WD)*, pp. 1–6, 2016.
- [13] M. F. Moller et al., "A scaled conjugate gradient algorithm for fast supervised learning," *Neural Networks*, 6(4), pp. 525–533, 1993.
- [14] YD. Bultitude et al., "T. IST-4-027756 WINNER II D1. 1.2 V1. 2 WINNER II Channel Models," Tech. Rep., Tech. Rep. 2007.